Evidence for Core-Shell Magnetic Behavior in Antiferromagnetic Co_3O_4 Nanowires

M. J. Benitez,[1,2,*] O. Petracic,[1,+] E. L. Salabas,[2] F. Radu,[3] H. Tüysüz,[2] F. Schüth,[2] and H. Zabel[1]

[1]*Institut für Experimentalphysik/Festkörperphysik, Ruhr-Universität Bochum, D-44780 Bochum, Germany*

[2]*Max-Planck Institut für Kohlenforschung, D-45470 Mülheim an der Ruhr, Germany*

[3]*BESSY GmbH, Albert-Einstein Strasse 15, D-12489 Berlin, Germany*

(Received 20 June 2008; published 29 August 2008)

Employing magnetometry measurements, we have studied Co_3O_4 nanowires focusing on the core-shell behavior. We find two magnetic contributions, i.e., a regular antiferromagnetic and an additional irreversible one. The first contribution can be attributed to the antiferromagnetically ordered wire cores. The nature of the second one can be identified using thermoremanent and isothermoremanent magnetizaton curves as magnetic fingerprints of the irreversible magnetization. We conclude that the nanowire shell behaves like a two-dimensional diluted antiferromagnet in a field.

DOI: 10.1103/PhysRevLett.101.097206 PACS numbers: 75.75.+a, 62.23.Hj, 75.50.Ee, 75.50.Lk

Magnetic nanoparticles and nanowires have attracted much interest among magnetism researchers for decades. This is not only due to their huge potential in technological applications in purely magnetic areas such as recording technology [1], but also in other disciplines such as biology and medicine [2]. In fundamental research they usually serve as ideal model systems, in particular, e.g., the Stoner-Wohlfarth and Néel-Brown model [3], or to study the finite-size effect [4]. The latter one is, in particular, relevant for nanoparticles and nanowires consisting of an antiferromagnetic (AFM) material. As the size of a magnetic system decreases, the significance of the surface spins increases. Since an antiferromagnet usually has two mutually compensating sublattices, the surface always leads to a breaking of the sublattice pairing and thus leads to ''uncompensated'' surface spins. This effect was already discussed by Néel for the explanation of a net magnetic moment in AFM nanoparticles [5]. Several experimental studies followed suggesting various scenarios for the magnetic properties found, e.g., spin-glass or cluster-glass-like behavior of the surface spins [6–9], thermal excitation of spin-precession modes [10], finite-size induced multisublattice ordering [11], core-shell interactions [7,8,12], or weak ferromagnetism [13,14]. However, the precise identification of the nature of the surface contribution has remained unclear. Terms like ''disordered surface state,'' ''loose surface spins,'' ''uncoupled spins,'' ''spin-glass-like behavior,'' etc. express the uncertainty in the description of the shell contribution. With the motivation to explicitly investigate the surface spin contribution in AFM nanosystems, we have synthesized high-quality AFM Co_3O_4 nanowires and performed magnetometry studies with emphasis on the thermoremanent magnetization (TRM) and isothermoremanent magnetization (IRM) curves. We show that the TRM/IRM curves can serve generally as ''fingerprints'' for the irreversible magnetization contribution in a disordered system. We identify the shell behavior as a diluted AFM in a field (DAFF), which is well known as a realization of a random field system [15].

Nanowires of Co_3O_4 were obtained using the nanocasting method [16]. We used as a template the two-dimensional hexagonal silica SBA-15, because it is a high-quality mesoporous material with a pore size easily tuned using hydrothermal treatments [17,18]. In our case 5 g of SBA-15 aged at 100 °C were mixed with 57 ml of 0.8 M solution of $Co(NO_3)_2{}^*6H_2O$ in ethanol and stirred for 2 h at room temperature. After the ethanol was removed by evaporation at 80 °C overnight, the sample was heated at 200 °C for 6 h. The impregnation procedure was repeated, followed by calcination at 450 °C for 6 h. To remove the template we use 125 ml of 2 M NaOH solution. The material synthesized has a Brunauer-Emmett-Teller (BET) surface area of 114 $m^2\,g^{-1}$ and pore volume reaching 0.17 $cm^3\,g^{-1}$. To confirm that the nanocasted wires are free of template, energy dispersive x-ray analysis studies were performed. We find less than 1% of Si in the Co_3O_4. The nanowires have a diameter of 8 nm and an average length of 50 nm estimated from high resolution transmission electron microscopy (HRTEM) and high resolution scanning electron microscopy (HRSEM) studies (Fig. 1). X-ray Rietveld refinement shows a single phase of Co_3O_4 with space group $Fd\bar{3}m$ in good agreement with Ref. [19]. Magnetic properties of the sample have been measured using a commercial superconducting quantum interference

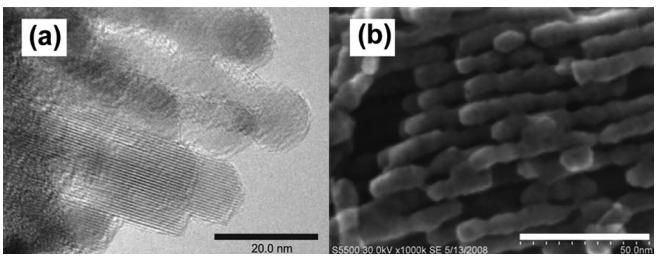

FIG. 1. HRTEM (a) and HRSEM (b) image of the Co_3O_4 nanowires after removal of the template. The average diameter of the wires is 8 nm and the average length 50 nm. The bar corresponds to 20 and 50 nm, respectively.

device (SQUID) magnetometer (MPMS, Quantum Design), in applied magnetic fields up to 50 kOe.

Figure 2 shows M vs T curves after zero field cooling (ZFC) and after field cooling (FC) measured at two applied fields, 40 kOe [2(a)] and 50 Oe [2(b)]. In each case the sample was cooled down from room temperature to 5 K. One finds two characteristic features. First, a bifurcation of the FC and ZFC magnetization below a temperature T_{bf}, which is a typical feature of spin glass, superparamagnetic (SPM), or DAFF behavior. In general, it signifies irreversible (''nonergodic'') contributions. Second, a peak in the ZFC curve is found, which usually signifies spin glass, superparamagnetic, or simply AFM behavior.

A regular nondiluted bulk AFM shows a peak when the field is applied along the anisotropy direction. The inflection point to the left of the peak position then marks the critical temperature $T_c(H)$, with $T_c(0) = T_N$. The peak position in the ZFC curve marks the onset of AFM long-range order and is also often considered to mark the critical temperature T_N. In order to be consistent with other literature we adopt the ZFC peak for the T_N definition.

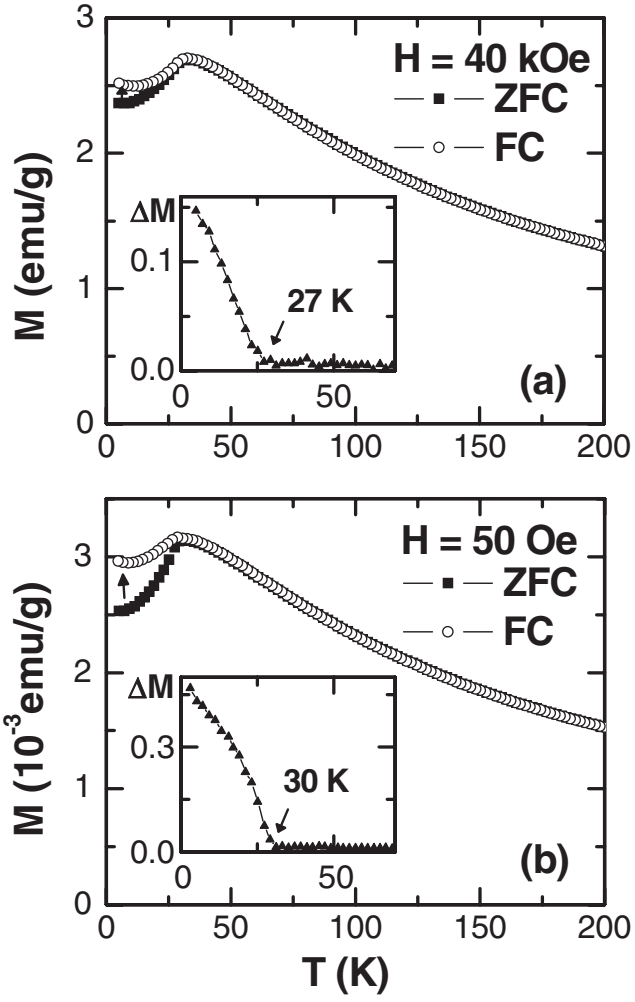

FIG. 2. M vs T curves after zero field cooling (ZFC) and after field cooling (FC) measured at two applied fields, i.e., 40 kOe (a) and 50 Oe (b). The insets show $\Delta M = M_{FC} - M_{ZFC}$. The bifurcation temperature T_{bf} is marked by an arrow.

In most AFM systems the field dependence of the critical phase boundary is very small in the range of the usually accessible experimental field values, i.e., $H < 50$ kOe. Therefore, the ZFC peak position is not expected to show any significant shift with increasing field. This matches well with the observation seen in Fig. 2. Comparing the ZFC curves for 40 kOe and 50 Oe, one finds virtually no change of the peak position ($T_N \approx 31$ K). Note that the Néel temperature of the nanowires is reduced compared to the bulk value of $T_N = 40$ K due to the finite-size effect [4,20]. From this finding we conclude that the Co_3O_4 wires consist of AFM ordered cores, which behave purely AFM. Hence, we can rule out SPM behavior of the entire nanowires. In a SPM system the peak positions, marking the blocking temperature, would show a much stronger shift with increasing field [3].

By plotting the difference between the magnetization curves, $\Delta M = M_{FC} - M_{ZFC}$ (Fig. 2, insets) only the irreversible contributions are displayed. One finds monotonically decreasing curves reflecting the expected thermally induced decay of magnetization. The ΔM curves reach zero at $T_{bf} = 27$ K (FC in 40 kOe) and $T_{bf} = 30$ K (FC in 50 Oe), which matches roughly with the ZFC peak positions. The reduced value for the 40 kOe data already hints toward a second magnetic subsystem—most probably a shell—having another temperature and field behavior compared to the nanowire cores.

In order to identify the shell contribution further magnetometry studies were performed. The presence of the memory effect [21–23] has been checked, which would be an indicator for spin-glass behavior of the wire shells. The ZFC curve has been recorded after cooling the sample from room temperature in zero field to 5 K with an intermediate halt of 12 h duration at $T = 20$ K. When this curve is subtracted from a regular ZFC curve without intermediate halt, then a spin-glass system would exhibit a peak at the halt temperature in the difference curve [22,23]. However, such a peak is absent in our data. This implies either that the shells do not show any spin-glass behavior or that the signal was too weak. However, estimating the surface-to-core ratio of the material, i.e., approximately 0.15 [24], and considering the overall large signal in the SQUID data, one can exclude the possibility that the signal from the wire surfaces is too small. Consequently, spin-glass behavior of the shells can be excluded.

Next we recorded hysteresis loops. Figure 3 shows $M(H)$ curves measured at 5 K after ZFC or FC in 40 kOe. The ZFC curve is point symmetric with a very small coercivity of 110 Oe and a virtually linear shape in the field range used. Such a curve is expected from a regular AFM system, again confirming that the dominant contribution is due to the AFM ordered wire cores. The

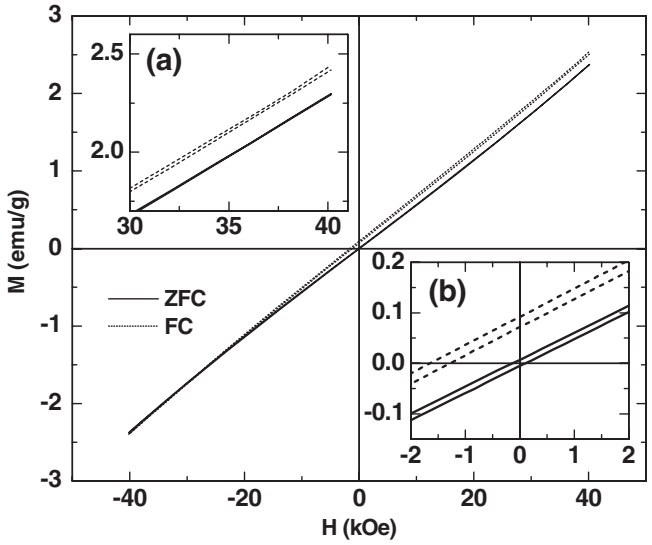

FIG. 3. M vs H curves at 5 K after ZFC and after FC. The insets show (a) an enlarged view at 40 kOe and (b) of the central part.

hysteresis curve measured after FC in 40 kOe displays an enhancement of the coercive field to 185 Oe. Moreover, one finds a vertical shift to larger $M(H)$ values. The consequence of the vertical shift is to observe also a horizontal one [see inset (b) in Fig. 3]. This might lead to the interpretation that an exchange bias effect is present [25]. However, comparing the ZFC and FC curves to those from a diluted bulk AFM, e.g., $Fe_{1-x}Zn_xF_2$ [26], one finds a compelling similarity which thus leads to a much more straightforward scenario in our AFM nanowires. We assume that the shell behaves like a DAFF system by virtue of its natural surface roughness; i.e., any roughness directly relates to a "dilution" (i.e., missing magnetic sites) at the surface.

In order to check this idea we performed measurements of the TRM and IRM vs H at 5 K in the field range 50 Oe $\leq H \leq$ 50 kOe. To measure the TRM the system was cooled in the specified field from room temperature down to 5 K, the field is removed, and then the magnetization recorded. To measure the IRM the sample was cooled in zero field from room temperature down to 5 K, the field was then momentarily applied, removed again, and the remanent magnetization recorded. It is important to note that the TRM and the IRM probe two different states. The TRM probes the remanent magnetization in zero field after freezing in a certain magnetization in an applied field during FC. However, the IRM probes the remanent magnetization in zero field after ZFC (in a demagnetized state) and magnetizing the system at low temperatures. Therefore, systems with a nontrivial H-T-phase diagram will show a characteristic difference between TRM and IRM. For example, the spin-glass state strongly depends on whether it is cooled in a field or not [27]. In contrast, a diluted antiferromagnet falls in two different universality classes: in zero field it behaves like a random exchange system, whereas in not too large applied fields it behaves like a random field system [15,26,28]. In the latter case a metastable domain state is frozen in during FC [29]. Therefore, we assume that by comparing the TRM/IRM plots for our system with those of, e.g., spin-glass and DAFF systems one can draw conclusions about the behavior in the Co_3O_4 nanowires.

Figure 4 shows the TRM and IRM curves as function of magnetic field 4(a) for our Co_3O_4 nanowires, 4(b) for the canonical spin-glass system AuFe adapted from Ref. [30], and 4(c) for the bulk-DAFF system, $Fe_{1-x}Zn_xF_2$, adapted from Ref. [26]. In the case of a spin glass [4(b)] one observes two features. First, the IRM increases relatively strongly with increasing field, then meets the TRM curve at moderate field values, where both then saturate. Second, the TRM exhibits a characteristic peak at intermediate fields, which is also reproduced from several other studies found in the literature [31,32]. This feature, which is surprising in itself, is to our knowledge absent in other systems. A superparamagnetic system shows a qualitatively similar plot, however, without this characteristic peak in the TRM curve [33].

We find no similarity of our Co_3O_4 nanowires [4(a)] to the one of 4(b). In our case the IRM stays at very small values even for fields up to 50 kOe, whereas the TRM curve shows a monotonic increase starting to saturate at approximately 50 kOe. Hence, one can exclude again the possibility of spin glass and also superparamagnetic behavior. However, comparing to the TRM/IRM plot of a DAFF system [4(c)] we find good correspondence. The bulk-DAFF system is characterized by a virtually zero IRM and a monotonically increasing TRM. The solid line in 4(c) is a fit to the TRM data according to the power law, TRM $\propto H^{\nu_H}$ [34], with $\nu_H = 3.05$ [26]. The TRM of the Co_3O_4 nanowires also displays a monotonically increasing curve, however with $\nu_H = 0.42$ [4(a)]. The TRM value is considered as a characteristic quantity of random field systems.

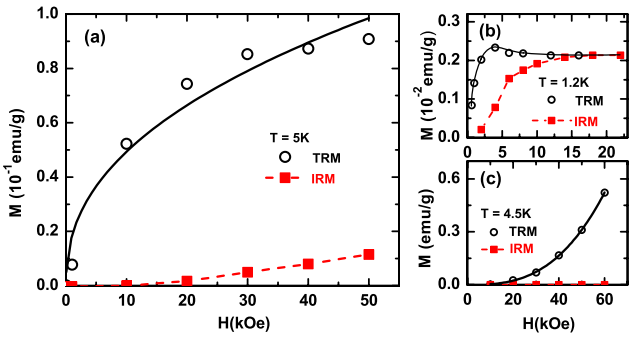

FIG. 4 (color online). TRM and IRM vs H (a) of Co_3O_4 nanowires at 5 K. The solid (black) line represents a fit to a power law, TRM $\propto H^{\nu_H}$. The broken (red) line is a guide to the eye. (b) TRM/IRM plot of the spin-glass system AuFe(0.5%) adapted from Ref. [30] and (c) of the DAFF system $Fe_{0.48}Zn_{0.52}Fe$, adapted from Ref. [26].

Theoretical studies on the 3D random field Ising model predict an inverse proportionality between TRM and the domain size, i.e., TRM $\propto R^{-1}$ with $R \propto H^{-\nu_H}$ [34,35]. We assume that the dimensionality and the finite size of the DAFF system play a crucial role in the TRM/IRM behavior and, in particular, the field dependence of the TRM so that a 2D finite-size DAFF system is likely to show a TRM vs H behavior as found in the Co_3O_4 nanowires. To the best of our knowledge, no such theoretical study is yet published in the literature for comparison. We argue that the TRM/IRM behavior of the Co_3O_4 shells corresponds more to DAFF than to the spin glass. However, a crossover from DAFF to spin-glass behavior in the shells might be observed [26], when the feature size is reduced or the disorder increased.

In summary, we present magnetometry studies on AFM Co_3O_4 nanowires with emphasis on the core-shell behavior. We show that the properties of the Co_3O_4 nanowires are governed by a regular AFM behavior from the wire cores. The irreversible magnetization contribution is due to wire shells, which behave as a 2D finite-size DAFF system. Although this interpretation is drawn only for this particular system, it might still be useful for reinterpreting previous results on other experimental AFM nanosystems. Moreover, we show that the TRM/IRM plot can serve generally as a ''fingerprint'' for irreversible magnetization contributions in disordered systems.

We thank B. Spliethoff for the HRTEM images, H. Bongard for the HRSEM images and energy dispersive x-ray analysis, and A. Cepak for help with the x-ray Rietveld refinement. One of the authors (M. J. B.) acknowledges support from the International Max-Planck Research School ''SurMat.''

*Maria.BenitezRomero@ruhr-uni-bochum.de
+oleg.petracic@ruhr-uni-bochum.de

[1] B. D. Terris and T. Thomson, J. Phys. D **38**, R199 (2005).
[2] A. K. Gupta and M. Gupta, Biomaterials **26**, 3995 (2005).
[3] J. L. Dormann, D. Fiorani, and E. Tronc, Adv. Chem. Phys. **98**, 283 (1997).
[4] X. Batlle and A. Labarta, J. Phys. D **35**, R15 (2002); X. G. Zheng, C. N. Xu, K. Nishikubo, K. Nishiyama, W. Higemoto, W. J. Moon, E. Tanaka, and E. S. Otabe, Phys. Rev. B **72**, 014464 (2005).
[5] L. Néel, Comptes Rendus **252**, 4075 (1961).
[6] S. D. Tiwari and K. P. Rajeev, Phys. Rev. B **72**, 104433 (2005).
[7] E. L. Salabaş, A. Rumplecker, F. Kleitz, F. Radu, and F. Schüth, Nano Lett. **6**, 2977 (2006).
[8] E. Winkler, R. D. Zysler, M. Vasquez Mansilla, and D. Fiorani, Phys. Rev. B **72**, 132409 (2005).
[9] J. B. Yi, J. Ding, Y. P. Feng, G. W. Peng, G. M. Chow, Y. Kawazoe, B. H. Liu, J. H. Yin, and S. Thongmee, Phys. Rev. B **76**, 224402 (2007).
[10] S. Moerup and C. Frandsen, Phys. Rev. Lett. **92**, 217201 (2004).
[11] R. H. Kodama, S. A. Makhlouf, and A. E. Berkowitz, Phys. Rev. Lett. **79**, 1393 (1997).
[12] J. Nogués, J. Sort, V. Langlais, V. Skumryev, S. Surinach, J. S. Munoz, and M. D. Baró, Phys. Rep. **422**, 65 (2005).
[13] A. Tomou, D. Gournis, I. Panagiotopoulos, Y. Huang, G. C. Hadjipanayis, and B. J. Kooi, J. Appl. Phys. **99**, 123915 (2006).
[14] A. Punnoose and M. S. Seehra, J. Appl. Phys. **91**, 7766 (2002).
[15] S. Fishman and A. Aharony, J. Phys. C **12**, L729 (1979).
[16] A. H. Lu and F. Schüth, Adv. Mater. **18**, 1793 (2006).
[17] A. Rumplecker, F. Kleitz, E. L. Salabaş, and F. Schüth, Chem. Mater. **19**, 485 (2007).
[18] M. Choi, W. Heo, F. Kleitz, and R. Ryoo, Chem. Commun. (Cambridge) 12 (2003) 1340.
[19] W. L. Roth, J. Phys. Chem. Solids **25**, 1 (1964).
[20] L. He, C. Chen, N. Wang, W. Zhou, and L. Guo, J. Appl. Phys. **102**, 103911 (2007).
[21] K. Jonason, E. Vincent, J. Hammann, J. P. Bouchaud, and P. Nordblad, Phys. Rev. Lett. **81**, 3243 (1998).
[22] P. E. Jönsson, Adv. Chem. Phys. **128**, 191 (2004).
[23] O. Petracic, X. Chen, S. Bedanta, W. Kleemann, S. Sahoo, S. Cardoso, and P. P. Freitas, J. Magn. Magn. Mater. **300**, 192 (2006).
[24] F. Radu *et al.* (unpublished).
[25] S. A. Makhlouf, J. Magn. Magn. Mater. **246**, 184 (2002).
[26] F. C. Montenegro, S. M. Rezende, and M. D. Coutinho-Filho, Rev. Bras. Fis. **21**, 192 (1991).
[27] J. A. Mydosh, *Spin Glasses: An Experimental Introduction* (Taylor & Francis, London, 1993).
[28] *Recent Progress in Random Magnets*, edited by D. H. Ryan (World Scientific, Singapore, 1992).
[29] W. Kleemann, Int. J. Mod. Phys. B **7**, 2469 (1993).
[30] J. L. Tholence and R. Tournier, J. Phys. (Paris), Colloq. **35**, C4-229 (1974).
[31] W. Kinzel, Phys. Rev. B **19**, 4595 (1979).
[32] K. Binder and A. P. Young, Rev. Mod. Phys. **58**, 801 (1986).
[33] R. M. Roshko, C. A. Viddal, S. Ge, and M. Gao, IEEE Trans. Magn. **40**, 2137 (2004).
[34] J. Villain, Phys. Rev. Lett. **52**, 1543 (1984).
[35] A. P. Malozemoff, Phys. Rev. B **37**, 7673 (1988).